

Cite this: *Dalton Trans.*, 2024, **53**, 15849

Low coordinate Zn(II) organocations bearing extremely bulky NHC ligands: structural features, air-/water-tolerance and use in hydrosilylation and hydrogenation catalysis†

Xuejuan Xu, Jordan Parmentier,  Christophe Gourlaouen,  Béatrice Jacques and Samuel Dagorne *

This work details the synthesis and characterization of low-coordinate Zn(II)-based organocations [(NHC)Zn(R)]⁺ incorporating extremely bulky NHCs [ITr] and [IAd] ([ITr] = [(ITr) = [(HCNCPh₃)₂C:]; [IAd] = [(HCNAd)₂C:]; Ad = adamantyl). Their structural features and particularities are thoroughly assessed as well as their air and water tolerance. Neutral ITr and IAd adducts [(ITr)Zn(R)₂] (**1**, R = Me; **2**, R = Et) and [(IAd)Zn(R)₂] (**3**, R = Me; **4**, R = Et) were synthesized by reaction of carbene [ITr] or [IAd] with a stoichiometric amount of [ZnR₂] and isolated in good yields. Despite the steric bulk of [ITr] and [IAd], neutral compounds **1–4** are robust and the solid state structure of adduct **3** was established through X-ray crystallographic studies as a trigonal monomer Zn(II) species. Adducts **1–4** may readily be ionized by [Ph₃C][B(C₆F₅)₄] to afford two-coordinate Zn(II) alkyl cations [(ITr)Zn(Me)]⁺ (**5**)⁺ and [(ITr)Zn(Et)]⁺ (**6**)⁺, [(IAd)Zn(Me)]⁺ (**7**)⁺ and [(IAd)Zn(Et)]⁺ (**8**)⁺, all isolated in high yields (>80%) as [B(C₆F₅)₄][−] salts, which were fully characterized. Remarkably, cation [(ITr)Zn(C₆F₅)]⁺ (**9**)⁺, prepared by reaction of **5**[B(C₆F₅)₄] with [B(C₆F₅)₃], features π–arene interactions with the electrophilic Zn(II), as deduced from solid state data and further completed by DFT-estimated non-covalent interactions (NCI), indicating that [ITr] may provide substantial steric and electrostatic stabilization. The latter certainly explains the remarkable stability of [(ITr)Zn(C₆F₅)]⁺ (**9**)⁺ towards hydrolysis at RT, as it only coordinates H₂O to afford an unprecedented stable Zn–OH₂ organocation **10**)⁺. Also noteworthy, H₂O coordination is reversible allowing recovery of [(ITr)Zn(C₆F₅)]⁺ cation, even after prolonged air exposure. Yet, controlled hydrolysis of [(ITr)Zn(C₆F₅)]⁺ may occur upon heating with selective protonolysis of the Zn–C₆F₅ bond to afford structurally characterized dication [(ITr)Zn(OH)]₂²⁺ (**11**)²⁺. Interestingly, despite steric hindrance, the air-/water-tolerant cation [(ITr)Zn(C₆F₅)]⁺ is an effective CO₂ hydrosilylation catalyst, and was also shown to mediate imine hydrogenation catalysis.

Received 26th July 2024,
Accepted 11th September 2024
DOI: 10.1039/d4dt02152e
rsc.li/dalton

Introduction

Thanks to their exceptional electronic and steric properties, *N*-heterocyclic carbenes (NHCs) have become a ubiquitous class of supporting ligands over the past 30 years for the stabilization of various metal/heteroatom complexes across fundamental organometallic chemistry and their applications, most notably catalysis.^{1–5} In particular, the strong σ-donation of NHCs along with their steric tunability has allowed the stabi-

lization/isolation of novel reactive organometallic moieties of potential interest for small molecules activation/functionalization, frequently in a catalytic manner.^{6–11}

Though first reported in the early 1990s,¹² Zn(II) organocations have received increased attention over the past ten years as well-defined Lewis acidic organometallics able to mediate the catalytic functionalization of various small molecules.¹³ In particular, the enhanced stability of NHC-stabilized Zn organocations has recently opened the way to numerous Zn-catalyzed transformations including hydrosilylation of unsaturated substrates (alkenes, alkynes, ketones and CO₂), allylic alkylation, alkyne hydroboration, alkyne dehydroboration/diboration, C–H borylation of heteroarenes.^{14–18} In this regard, we earlier reported that two-coordinate Zn(II) organocations of the type [(NHC)Zn(R)]⁺ (R = alkyl, aryl) are stable species despite enhanced electrophilicity and Lewis acidity at Zn(II), and

Institut de Chimie (UMR CNRS 7177), CNRS – Université de Strasbourg, 4, rue Blaise Pascal, 67000 Strasbourg, France. E-mail: dagorne@unistra.fr

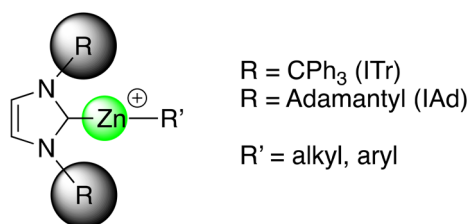
† Electronic supplementary information (ESI) available: NMR spectra, crystallographic details, DFT calculation details. CCDC 2372716–2372720 and 2373743. For ESI and crystallographic data in CIF or other electronic format see DOI: <https://doi.org/10.1039/d4dt02152e>



behave as effective catalysts for CO₂, alkene/alkyne/ketone hydrosilylation and alkyne hydroboration.^{18–20} Yet, the limited hydrolytic and thermal stability of [(NHC)Zn(R)]⁺ cations thus far prepared led us to the development of novel classes of [(NHC)Zn(R)]⁺ cations for a broader use in catalysis and polar substrates activation. We earlier observed that *bulky-yet-flexible* NHC ligand [IPr*] may provide a limited, though improved, hydrolytic stability of the resulting [(NHC)Zn(R)]⁺ cation, but it came along with a poor thermal stability above room temperature.²⁰

For more robust [(NHC)Zn-R]⁺ systems, the use of extremely sterically bulky NHCs, such as [ITr] and [IAd] carbenes (Fig. 1), was envisaged. Though little used for coordination chemistry, the [ITr] carbene was shown to stabilize low-coordinate metal cations, including two-coordinate Ge(II) and monocoordinate Ag(I) cations.^{21,22} While the present study was ongoing, [ITr]-stabilized Zn(II) halides were also reported to exhibit phosphorescence properties.²³ Besides steric protection, possible arene π -interactions between [ITr] (the *N*-CPh₃ phenyl groups) and the cationic Zn(II) center may also contribute to the stabilization of [(NHC)Zn-R]⁺ cations. In this regard, arene π -stabilization of a cationic Zn center was recently observed for several low-coordinate Zn(II) cations.^{24–26}

We herein report on the synthesis and structure of [(NHC)Zn(R)]⁺ organocations (NHC = ITr, IAd; R = alkyl, aryl; Fig. 1) and their reactivity in the presence of H₂O and/or air, along with characterization of the products derived from. The performances of the most robust Zn(II) system in CO₂ hydrosilylation and imine hydrogenation catalysis are also discussed.



Extremely bulky Zn cations for air and water tolerance

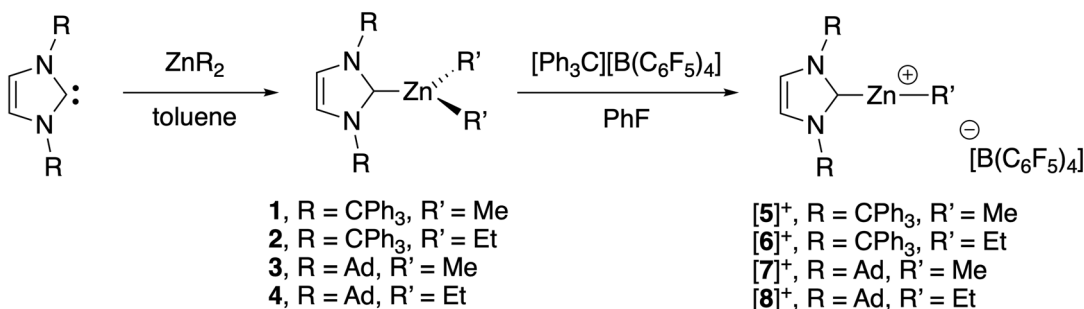
Fig. 1 Studied extremely bulky [(NHC)Zn(R)]⁺ cations.

Results – discussion

Synthesis and structure of the ITr and IAd zinc alkyl complexes 1–4 and [5–8][B(C₆F₅)₄]

The preparation of targeted organocations [(ITr)Zn(R)]⁺ and [(IAd)Zn(R)]⁺ required the synthesis of corresponding neutral precursors [(ITr)Zn(R)₂] (R = Me, Et, 1–2; Scheme 1), [IAdZnR₂] (R = Me, Et, 3–4; Scheme 1), which were also fully characterized. Adducts 1–4 were synthesized by reaction of carbene [ITr] or [IAd], both prepared according to literature procedures,^{21,27} with one equiv. of [ZnR₂] (R = Me, Et) to afford adducts 1–4, all isolated in high yields as analytically pure colorless solids. NMR data are consistent with adduct formation with a characteristic upfield chemical shift of the C_{carbene} signal in 1–4 (ranging from 186.9 to 199.0 ppm *versus* 211.0 and 226.0 ppm for free [IAd] and [ITr], respectively),^{21,28} indicating effective NHC coordination to the Zn(II) center despite severe steric hindrance imposed by [ITr] and [IAd].²⁹ The solid state molecular structure of adduct 2 was established through X-ray crystallographic analysis and is depicted in Fig. 2. Adduct 2 consists of a monomeric ITr-stabilized three-coordinate center with a rather long Zn–C_{carbene} bond distance (2.154(2) Å) compared to that in [(IPr)ZnMe₂] (2.112(2) Å), presumably due to greater steric hindrance.²⁹ Yet, no short contacts are detected between the ITr moiety and ZnEt₂ fragments in adduct 2, with the shortest distances being close or above the sum of van der Waals radii of Zn and C_{sp²} atoms (3.10 Å).³⁰ In addition, in line with robust [(ITr)ZnR₂] adducts, the binding energy between [ITr] and [ZnEt₂] was estimated by DFT calculations (ω B97XD/6-31+G** theory level, $\Delta G = -8.2$ kcal mol⁻¹). Such adduct appears more stable than [(IPr)ZnEt₂] ($\Delta G = -2.1$ kcal mol⁻¹), which is probably due to stronger London dispersion interactions in adduct 2.

The Zn–alkyl cations [(ITr)Zn(R)]⁺ ([5]⁺, R = Me; [6]⁺, R = Et; Scheme 1) and [(IAd)Zn(R)]⁺ ([7]⁺, R = Me; [8]⁺, R = Et; Scheme 1) were prepared *via* alkyl abstraction of the corresponding neutral precursors 1–4, respectively. Thus, reaction of 1–4 with 1 equiv. of [Ph₃C][B(C₆F₅)₄] (PhF, 30 min to 1 h, RT) afforded organocations [5–8]⁺, which were all isolated in a pure form as [B(C₆F₅)₄]⁻ salts in high yields (79 to 92% yield). Salts [5–8][B(C₆F₅)₄] are stable for days in CD₂Cl₂ and for weeks in C₆D₅Br under inert atmosphere. ¹H, ¹³C and ¹⁹F NMR data for



Scheme 1 Synthesis of neutral and cationic Zn–NHC complexes.



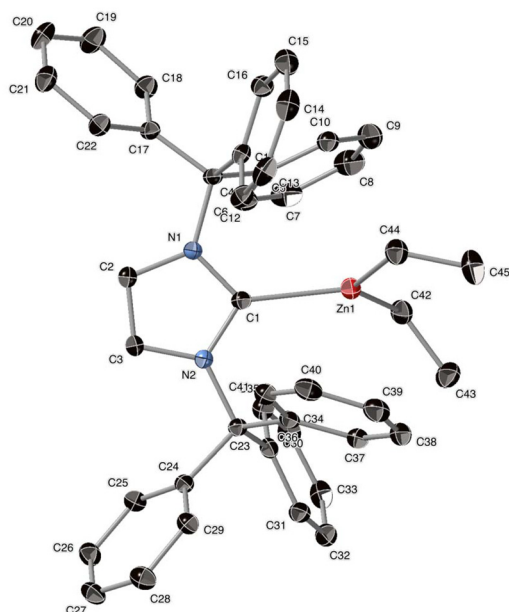


Fig. 2 Molecular structure (ORTEP view) of neutral adduct $[(\text{ITr})\text{ZnEt}_2]$ (**2**). Selected bond distances (Å) and angles ($^\circ$). $\text{Zn1}-\text{C1} = 2.154(2)$, $\text{C1}-\text{N1} = 1.367(2)$, $\text{C1}-\text{N2} = 1.368(2)$, $\text{Zn1}-\text{C42} = 2.018(2)$, $\text{Zn1}-\text{C44} = 2.012(2)$, $\text{C42}-\text{Zn1}-\text{C44} = 123.48(8)$, $\text{C44}-\text{Zn1}-\text{C1} = 116.76(7)$, $\text{C42}-\text{Zn1}-\text{C1} = 119.74(7)$.

all salts are consistent with the formation of $[(\text{NHC})\text{Zn}(\text{R})]^+$ -type cations with no observable cation/anion interactions in solution.³¹ For instance, in the case of $[\mathbf{6}]^+$, the $\text{C}_{\text{carbene}}$ ^{13}C NMR signal ($\delta = 172.6$ ppm) is significantly upfield shifted

versus that of neutral adduct **2** ($\delta = 199.0$ ppm), consistent with a more Lewis acidic $\text{Zn}(\text{II})$ center in $[\mathbf{6}]^+$.³²

The molecular structures of salts $[\mathbf{6}][\text{B}(\text{C}_6\text{F}_5)_4]$ and $[\mathbf{8}][\text{B}(\text{C}_6\text{F}_5)_4]$ were further established through X-ray crystallographic analysis. Both salts crystallize as discrete and fully dissociated $[(\text{ITr})\text{Zn}(\text{Et})]^+ / [(\text{IAd})\text{Zn}(\text{Et})]^+$ and $[\text{B}(\text{C}_6\text{F}_5)_4]^-$ ions, and the cations are depicted in Fig. 3. Both cations display overall similar structural and geometrical features, with a sp -hybridized, two-coordinate $\text{Zn}(\text{II})$ center with $\text{Zn}-\text{C}_{\text{carbene}}$ and $\text{Zn}-\text{alkyl}$ bond distances (1.957(3) and 1.927(4) Å average) and a $\text{C}_{\text{NHC}}-\text{Zn}-\text{Et}$ bond angle ($176.0(1)^\circ$ average) similar to those in cation $[(\text{IPr})\text{Zn}(\text{Me})]^+$.¹⁹ Noticeably, for cation $[\mathbf{6}]^+$, due to the enhanced Lewis acidity at the $\text{Zn}(\text{II})$ center and the presence of the $\text{N}-\text{CPh}_3$ substituents, two Ph groups point towards the metal center with short contacts ($\text{Zn1}\cdots\text{C36} = 2.882$ Å, $\text{Zn1}\cdots\text{C37} = 3.081$ Å) slightly below the sum of van der Waals radii of Zn and C_{sp^2} atoms (3.10 Å).³⁰ As shown in Fig. 3, even shorter contacts are observable for the $(\text{IAd})\text{Zn}$ cation $[\mathbf{8}]^+$ ($\text{Zn1}\cdots\text{C19} = 2.778$ Å, $\text{Zn1}\cdots\text{C5} = 2.853$ Å), reflecting severe steric crowding at the Zn center.

Synthesis and structure of cation $[(\text{ITr})\text{ZnC}_6\text{F}_5]^+$

The $\text{Zn}-\text{C}_6\text{F}_5$ cations $[(\text{ITr})\text{Zn}(\text{C}_6\text{F}_5)]^+$ ($[\mathbf{9}]^+$, Scheme 2) and $[(\text{IAd})\text{Zn}(\text{C}_6\text{F}_5)]^+$ were next targeted, since expected to be the most Lewis acidic of the series. The $\text{Me}/\text{C}_6\text{F}_5$ ligand exchange reaction between cation $[(\text{ITr})\text{Zn}(\text{Me})]^+$ with $[\text{B}(\text{C}_6\text{F}_5)_3]$ (1.5 equiv., PhF, 48 h, RT) quantitatively afforded cation $[(\text{ITr})\text{Zn}(\text{C}_6\text{F}_5)]^+$, which was isolated as $[\mathbf{9}][\text{B}(\text{C}_6\text{F}_5)_4]$ in 89% yield. In contrast, using similar or slightly modified reaction conditions, all attempted synthesis of the IAd cationic analogue

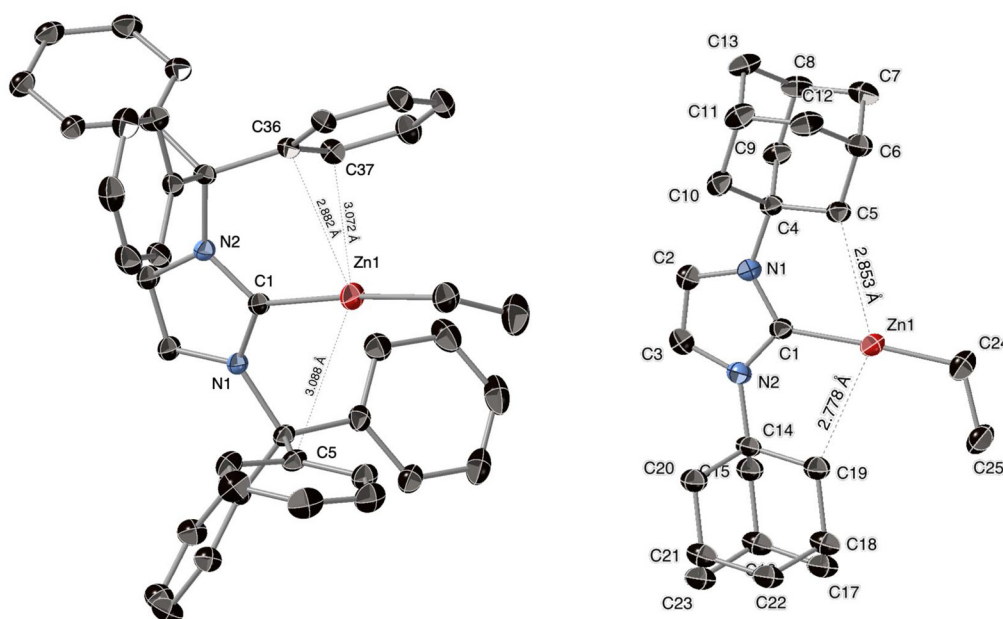
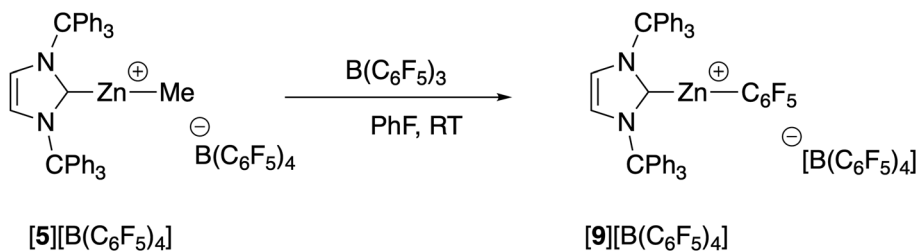


Fig. 3 Molecular structures (ORTEP views) of Zn cations $[(\text{ITr})\text{ZnEt}]^+$ ($[\mathbf{6}]^+$, left) and $[(\text{IAd})\text{ZnEt}]^+$ ($[\mathbf{8}]^+$, right). Selected bond distances (Å) and angles ($^\circ$). For $[\mathbf{6}]^+$: $\text{Zn1}-\text{C1} = 1.962(1)$, $\text{C1}-\text{N1} = 1.353(2)$, $\text{C1}-\text{N2} = 1.354(1)$, $\text{Zn1}-\text{C42} = 1.930(1)$, $\text{C42}-\text{Zn1}-\text{C1} = 175.30(6)$. For $[\mathbf{8}]^+$: $\text{Zn1}-\text{C1} = 1.953(2)$, $\text{C1}-\text{N1} = 1.354(2)$, $\text{C1}-\text{N2} = 1.359(2)$, $\text{Zn1}-\text{C24} = 1.925(2)$, $\text{C24}-\text{Zn1}-\text{C1} = 176.72(9)$.





Scheme 2 Synthesis of the [(ITr)Zn(C₆F₅)]⁺ cation.

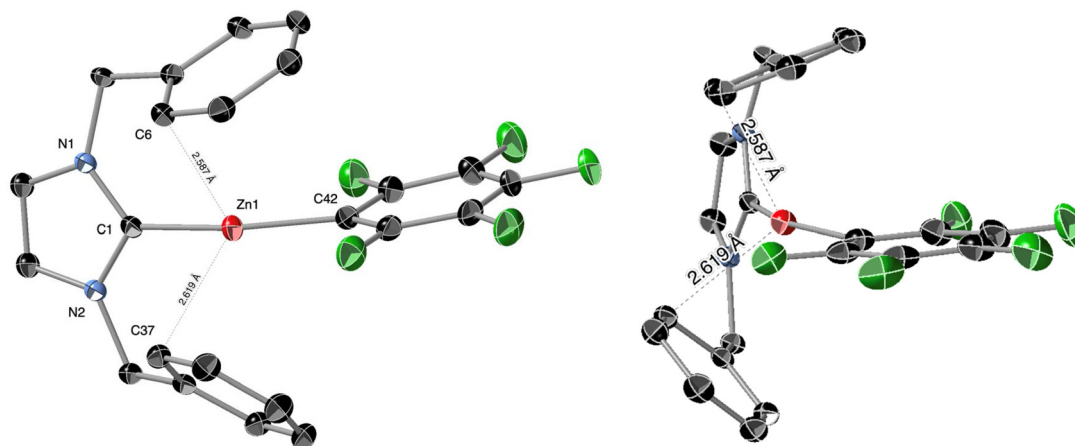


Fig. 4 Molecular structure (ORTEP view) of Zn cation [(ITr)Zn(C₆F₅)]⁺ ([9]⁺). Sideview on the left and frontview on the right. Two phenyls of each CPh₃ group are omitted for clarity. Selected bond distances (Å) and angles (°). Zn1–C1 = 1.963(2), C1–N1 = 1.345(2), C1–N2 = 1.355(2), Zn1–C42 = 1.938(1), Zn1...C6 = 2.587(1), C42–Zn1–C1 = 154.85(6).

[(IAd)Zn(C₆F₅)]⁺ were unsuccessful and only led to unidentified products. This may be due to the instability of cation [(IAd)Zn(C₆F₅)]⁺ for steric reasons.

As established through XRD analysis, salt [9][B(C₆F₅)₄] crystallizes as dissociated [9]⁺ and [B(C₆F₅)₄][−] ions, and the structure of [9]⁺ is shown in Fig. 4. Cation [9]⁺ indeed consists of a two-coordinate Zn(II) cation supported by a ITr ligand and a C₆F₅[−] X-type ligand. The geometrical/bonding parameters of [9]⁺ are broadly similar to those of the Zn–Et⁺ cation [6]⁺ discussed above. However, reflecting the stronger Lewis acidity of [9]⁺ versus [6]⁺, significantly shorter Zn...Ph π -interactions are observed in [9]⁺ (Zn1...C6 = 2.587 Å, Zn1...C37 = 2.619 Å; Fig. 4), suggesting the actual formation of a (η^1 -arene)₂Zn π -complex. Such interactions probably explain the significantly smaller NHC–Zn–C bond angle (154.85(6)°) in [9]⁺ compared to those in [6]⁺ (175.30(6)°) and [8]⁺ (176.72(9)°). For comparison, the observed Zn...Ph distances in [9]⁺ (2.603 Å average) are in a similar range to those in the benzene complex [(Et)Zn(η^3 -benzene)][CHB₁₁Cl₁₁] (2.529 Å average)²⁴ and toluene complex [(Et)Zn(η^3 -toluene)₂][Al{OC(CF₃)₃]₄] (2.555 Å average),²⁵ but are longer than in [(BDI)Zn(η^2 -benzene)][B(C₆F₅)₄] (BDI = β -diketiminato, 2.380 Å average).²⁶

For further insight, DFT-estimated Non Covalent Interactions (NCI) of a model of cation [9]⁺, IX (Fig. 5), further confirm attractive interactions including dispersion forces

(light green basins) and electrostatic interactions (blue basins) between the Zn center and the two “sandwiching” Ph rings.

Lewis acidity of IAd-/ITr-stabilized Zn organocations

The Fluoride Ion Affinity (FIA) of Zn organocations [(IAd)Zn(Et)]⁺ ([8]⁺), [(ITr)Zn(Et)]⁺ ([6]⁺) and [(ITr)Zn(C₆F₅)]⁺ ([9]⁺) was calculated by DFT (B3LYP/6-31+G**, see ESI† for more details) to assess their Lewis acidity.³³ As previously validated and used in comparable systems involving Zn cations, such level of theory was found appropriate since it constitutes a reasonable compromise between accuracy and efficiency, allowing calculations on large systems at an acceptable cost/time.³⁴ According to FIA data, [(IAd)Zn(Et)]⁺ is the most Lewis acidic of all three evaluated cations ([8]⁺, FIA = 129.7 kJ mol^{−1}, [6]⁺, FIA = 102.1 kJ mol^{−1}; [9]⁺, FIA = 118.5 kJ mol^{−1}), indicating that the voluminous CPh₃ groups in the ITr moiety along with the π -arene–Zn interactions significantly quench the Lewis acidity of the Zn center in (ITr)Zn cations. In line with the latter, the Lewis acidity of [(ITr)Zn(C₆F₅)]⁺ ([9]⁺) is also significantly lower than that of benchmark [(IPr)Zn(C₆F₅)]⁺ cation (FIA = 156 kJ mol^{−1}).¹⁹ The larger FIA for the (IAd)Zn alkyl cation [8]⁺ vs. and its ITr analogue [6]⁺ further indicates the superior stabilization of the Zn center provided by carbene [ITr].



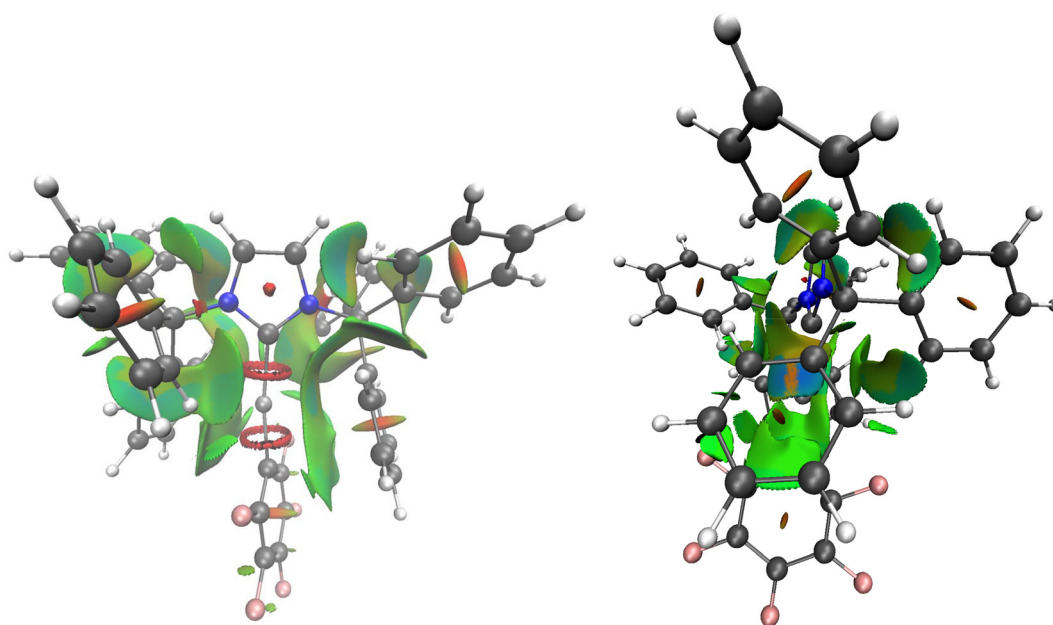


Fig. 5 Non covalent interactions (NCI) isosurface ($h = 0.65$) for model cation $[(\text{ITr})\text{Zn}(\text{C}_6\text{F}_5)]^+$ (VI), as estimated by DFT calculations at the $\omega\text{B97XD}/6\text{-31+G}^{**}$ theory level. Green areas correspond to attractive van der Waals interactions, blue areas indicate electrostatic interactions, and red areas indicate repulsive steric congestion.

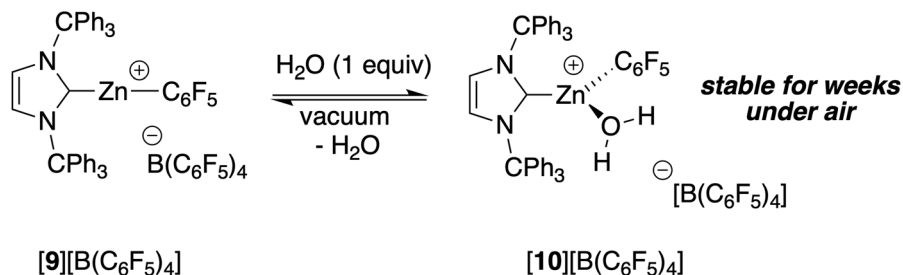
Reactivity of cation $[(\text{ITr})\text{Zn}(\text{C}_6\text{F}_5)]^+$ with H_2O and air stability

A primary goal of the present study was to access $[(\text{NHC})\text{Zn}(\text{R})]^+$ cation with significantly improved stability under and/or under hydrolytic conditions. Initial studies on the reaction of the Zn-alkyl cations $[(\text{ITr})\text{Zn}(\text{R})]^+$ ($[\mathbf{5}]^+$ and $[\mathbf{6}]^+$) with H_2O (1 equiv.) in $\text{C}_6\text{D}_5\text{Br}$ at room temperature immediately led to the formation of an intractable mixture of species (<15 min), among which methane/ethane and imidazolium $[\text{ITr}-\text{H}]^+$ could be identified. In contrast, the reaction of $[(\text{ITr})\text{Zn}(\text{C}_6\text{F}_5)]^+$ with 1 equiv. of H_2O ($\text{C}_6\text{D}_5\text{Br}$, room temperature) led to the immediate and quantitative formation of the cationic water adduct $[(\text{ITr})\text{Zn}(\text{C}_6\text{F}_5)(\text{OH}_2)]^+$ ($[\mathbf{10}]^+$, Scheme 3) as a dissociated $[\text{B}(\text{C}_6\text{F}_5)_4]^-$ salt, as deduced from ^1H , ^{13}C , ^{19}F , 2D HSQC and 2D HMBC NMR data (see ESI †). In particular, the ^1H NMR spectrum contains a characteristic Zn- OH_2 signal for two protons ($\delta = 2.33$ ppm) while ^{13}C and 2D NMR data are all consistent with the $(\text{ITr})\text{Zn}(\text{C}_6\text{F}_5)^+$ fragment retaining its integrity,

with the $\text{C}_{\text{carbene}}$ chemical shift of $[\mathbf{10}]^+$ being only slightly shifted upon H_2O coordination ($\delta = 168.8$ and 166.4 ppm for $[\mathbf{10}]^+$ and $[\mathbf{9}]^+$, respectively). To our knowledge, this is the first instance of a characterized stable water adduct of a Zn(II) organocation.

Remarkably, $[\mathbf{10}][\text{B}(\text{C}_6\text{F}_5)_4]$ is stable for weeks in CD_2Cl_2 or $\text{C}_6\text{D}_5\text{Br}$ under inert atmosphere, with no sign of decomposition after a month from ^1H NMR data. Interestingly, H_2O coordination to $[\mathbf{9}]^+$ appears reversible with the complete recovery of water-free cation $[\mathbf{9}]^+$ upon exposure of a solution of $[\mathbf{10}]^+$ under vacuum (2×10^{-3} mbar, overnight), which also unfortunately precluded the isolation of $[\mathbf{10}][\text{B}(\text{C}_6\text{F}_5)_4]$ in a pure form.

The air stability of salt $[\mathbf{9}][\text{B}(\text{C}_6\text{F}_5)_4]$ was also evaluated. Leaving solid $[\mathbf{9}][\text{B}(\text{C}_6\text{F}_5)_4]$ (colorless powder) for a month under air (open vial) at room temperature resulted in no visible change, but ^1H NMR data showed the complete and selective formation of water adduct $[\mathbf{10}][\text{B}(\text{C}_6\text{F}_5)_4]$, which was then converted back to $[\mathbf{9}][\text{B}(\text{C}_6\text{F}_5)_4]$ under vacuum. This indi-



Scheme 3 Air and hydrolysis stability of cation $[(\text{ITr})\text{Zn}(\text{C}_6\text{F}_5)]^+$.



cates that cation $[(\text{ITr})\text{Zn}(\text{C}_6\text{F}_5)]^+$ may be readily recovered without any alteration upon prolonged air exposure.

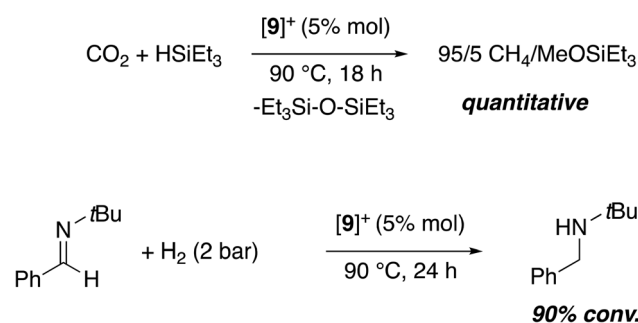
For further characterization of the cationic water adduct $[\mathbf{10}][\text{B}(\text{C}_6\text{F}_5)_4]$, its Brønsted acidity/ $\text{p}K_{\text{a}}$ value was also evaluated through DFT calculations ($\omega\text{B97XD}/6\text{-}31\text{+G}^{**}$ theory level). Estimations were done in MeCN (through a PCM) using a relative method involving an acid for which the $\text{p}K_{\text{a}}$ is experimentally known (see ESI† for further details). The $\text{p}K_{\text{a}}$ of cation $[\mathbf{10}]^+$ was computed to be around 21, thus indicating significantly more acidic water protons in $[\mathbf{10}]^+$ than those of free water (the $\text{p}K_{\text{a}}$ of H_2O in MeCN has been reported to lie between 38 and 41).³⁵ Therefore, despite ready decoordination of H_2O from $[\mathbf{10}]^+$ under vacuum, there is substantial H_2O activation by the Zn(II) cationic center in cation $[\mathbf{10}]^+$.

Though stable at room temperature, the water adduct $[\mathbf{10}][\text{B}(\text{C}_6\text{F}_5)_4]$ slowly reacts upon heating ($\text{C}_6\text{D}_5\text{Br}$, 60 °C, 24 h) to afford a 1/1 $\text{C}_6\text{F}_5\text{H}/[\mathbf{10}][\text{B}(\text{C}_6\text{F}_5)_4]$ mixture, in line with a 50% hydrolysis of the Zn– C_6F_5 bond in $[\mathbf{10}][\text{B}(\text{C}_6\text{F}_5)_4]$, as deduced from ^1H and ^{19}F NMR data (see ESI†). Crystallization of salt $[(\text{ITr})\text{Zn}(\mu\text{-OH})_2][\text{B}(\text{C}_6\text{F}_5)_4]_2$ ($[\mathbf{11}][\text{B}(\text{C}_6\text{F}_5)_4]_2$) as single crystals from the mixture (28% yield) led to its formulation after structure determination by XRD analysis, and elemental analysis. The poor solubility of salt $[\mathbf{11}][\text{B}(\text{C}_6\text{F}_5)_4]_2$ in common organic solvents, including CH_2Cl_2 , benzene, MeCN and THF, prevented any NMR characterization. Salt $[\mathbf{11}][\text{B}(\text{C}_6\text{F}_5)_4]_2$ crystallizes as fully dissociated $[(\text{ITr})\text{Zn}(\mu\text{-OH})_2]^{2+}$ ($[\mathbf{11}]^{2+}$) and $[\text{B}(\text{C}_6\text{F}_5)_4]^-$ ions, and the molecular structure of the Zn di-cation $[\mathbf{11}]^{2+}$ is shown in Fig. 6. Di-cation $[(\text{ITr})\text{Zn}(\mu\text{-OH})_2]^{2+}$ consists of a centrosymmetric dimer associating two $[(\text{ITr})\text{Zn}(\text{OH})]^+$ fragments *via* two $\mu\text{-OH}$ bridging hydroxides, and constitutes a unique example of structurally characterized $[(\text{NHC})\text{Zn}$

$(\text{OH})^+$ -type species.³⁶ The two NHC rings are coplanar and form an angle of 69.92° with the $[\text{Zn}_2\text{O}_2]$ central core plane. The Zn–O bond distances (Zn1–O1 = 1.907(2) Å, Zn1'–O1 = 1.938(2)) are in the normal range for Zn–O distances.

CO_2 hydrosilylation and imine hydrogenation catalysis by cation $[(\text{ITr})\text{Zn}(\text{C}_6\text{F}_5)][\text{B}(\text{C}_6\text{F}_5)_4]$ ($[\mathbf{9}][\text{B}(\text{C}_6\text{F}_5)_4]$)

Cation $[\mathbf{9}]^+$ was tested in CO_2 hydrosilylation catalysis given the importance of such transformation and the known ability of Lewis acids for functionalize CO_2 with hydrosilanes.³⁷ Though inactive at room temperature, cation $[\mathbf{9}]^+$ (5 mol%) reduces CO_2 (1.5 bar) to a 95/5 $\text{CH}_4/\text{MeOSiEt}_3$ ($\text{C}_6\text{D}_5\text{Br}$, 90 °C) in the presence of HSiEt_3 (20 equiv. *vs.* $[\mathbf{9}][\text{B}(\text{C}_6\text{F}_5)_4]$) with complete silane conversion after 18 h (Scheme 4), a comparable activity to Zn cation $[(\text{IPr})\text{Zn}(\text{C}_6\text{F}_5)]^+$.¹⁹ In contrast, the less robust Zn-alkyl cations $[\mathbf{5}]\text{--}[\mathbf{8}]^+$ showed no activity under such conditions.



Scheme 4 CO_2 hydrosilylation and imine hydrogenation catalysis using $[\mathbf{9}][\text{B}(\text{C}_6\text{F}_5)_4]$.

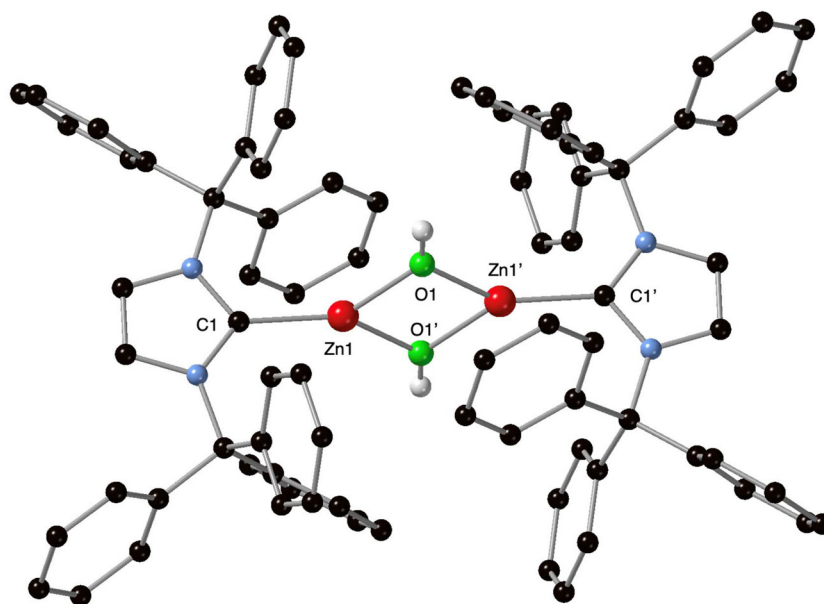


Fig. 6 Molecular structure of Zn dication $[(\text{ITr})\text{Zn}(\mu\text{-OH})_2]^{2+}$ ($[\mathbf{11}]^{2+}$). Selected bond distances (Å) and angles (°). Zn1–C1 = 1.980(2), C1–N1 = 1.361(3), C1–N2 = 1.356(3), Zn1–O1 = 1.907(2), Zn1'–O1 = 1.938(2), O1–Zn1–C1 = 146.30(8), O1–Zn1–O1' = 80.16(8), Zn1–O1–Zn1' = 99.84(8).



Based on ^1H and ^{19}F NMR monitoring as the catalysis proceeds, cation $[9]^+$ retained its integrity till the end of the reaction, in line with a Lewis-acid-type mechanism.¹⁹

Lewis acidic cation $[9]^+$ was tested in imine hydrogenation catalysis, as hydrogenation catalysis mediated by discrete and well-defined Zn(II) species remains little explored.^{38–41} In the presence of cation $[9]^+$ (5 mol%) and H_2 (2 bar), aldimine $\text{PhCH}=\text{N}t\text{Bu}$ is hydrogenated to the corresponding amine $\text{PhCH}_2\text{-NH}t\text{Bu}$ (90% NMR yield, $\text{C}_6\text{D}_5\text{Br}$, 90 °C) after 24 h of reaction, as deduced from NMR spectroscopic data. For comparison, benchmark cation $[(\text{IPr})\text{Zn}(\text{C}_6\text{F}_5)]^+$ showed no catalytic activity under identical conditions. As monitored by ^1H and ^{19}F NMR, cation $[9]^+$ gradually decomposes to unknown species over the course of imine hydrogenation catalysis (24 h), complicating any clear-cut mechanistic proposal on the hydrogenation reaction. Yet, the involvement/formation of transient Zn–H species that would form from cation $[9]^+$ appears required for imine hydrogenation, as has been observed in several imine hydrogenation catalysed by Zn complexes.^{38–41} In the present case, Frustrated Lewis Pair type reactivity is likely to operate with, under catalytic conditions, a heterolytic splitting of H_2 by an *in situ* formed $[9]^+$ / $\text{PhCH}=\text{N}t\text{Bu}$ Lewis pair resulting into the transient neutral Zn–H species $[(\text{ITr})\text{Zn}(\text{C}_6\text{F}_5)(\text{H})]$ along with iminium $[\text{PhCH}=\text{N}(\text{H})(t\text{Bu})]^+$, reminiscent of the reactivity of NHC/ Cp^*Zn Lewis pairs.³⁸ From there, $\text{PhCH}=\text{N}t\text{Bu}$ insertion in the Zn–H may proceed to form the corresponding Zn–amido species that may then undergo protolysis with the iminium moiety, producing the amine product and re-generating cation $[9]^+$. Alternatively, a direct hydride transfer from initially generated $[(\text{ITr})\text{Zn}(\text{C}_6\text{F}_5)(\text{H})]$ to iminium $[\text{PhCH}=\text{N}(\text{H})(t\text{Bu})]^+$ may also occur, generating the amine product and re-generate $[9]^+$.

Hartwig recently showed that catalytically active transient Zn–H species may be generated from Zn–OH moieties of carbonic anhydrase enzymes and hydrosilanes in water medium, systems that were successfully exploited for enantioselective ketone hydrosilylation catalysis.⁴² As potential Zn–OH sources, the cationic water adduct $[10]^+$ (generated *in situ*) and the Zn hydroxide dication $[(\text{ITr})\text{Zn}(\text{OH})_2]^{2+}$ ($[11]^{2+}$) were also tested in imine hydrogenation catalysis (5 mol% cat., $P_{\text{H}_2} = 2$ bar). Both cations displayed no catalytic activity after 24 h at 90 °C in $\text{C}_6\text{D}_5\text{Br}$. As monitored by ^1H and ^{19}F NMR, cation $[10]^+$ slowly converted to a $[\text{Zn}(\text{OH})]^+$ -type species, likely $[11]^{2+}$ over the course of the catalytic test, as deduced from the formation of hydrolysis product $\text{C}_6\text{F}_5\text{H}$. The presumed stability of dicationic dimer $[11]^{2+}$ against dissociation under the studied conditions may play a role in its lack of reactivity.

Conclusion

Two-coordinate Zn organocations $[(\text{NHC})\text{Zn}(\text{R})]^+$ bearing extremely bulky NHC ligands [ITr] and [IAd] were first prepared and characterized for improved robustness and hydrolytic stability. While IAd-stabilized Zn cations display a limited stability, possibly due to a too severe steric hindrance of adamantyl

groups at the Zn(II) center, [ITr] carbene is much better suited and leads to Zn(II) organocations with significantly increased robustness combining a voluminous steric protection of the Zn center and stabilization through the formation of arene...Zn π -bonding interactions. Thus, [ITr]-stabilized Zn cation $[(\text{ITr})\text{Zn}(\text{C}_6\text{F}_5)]^+$ is stable towards hydrolysis at RT, since only coordinating H_2O to afford an unprecedented stable cationic water adduct. Remarkably, H_2O coordination is reversible allowing recovery of $[(\text{ITr})\text{Zn}(\text{C}_6\text{F}_5)]^+$ cation, even after prolonged air exposure. Yet, controlled hydrolysis of $[(\text{ITr})\text{Zn}(\text{C}_6\text{F}_5)]^+$ may occur upon heating with the selective protonolysis of the Zn– C_6F_5 bond to afford structurally characterized dication $[(\text{ITr})\text{Zn}(\text{OH})_2]^{2+}$.

Despite steric hindrance, cation $[(\text{ITr})\text{Zn}(\text{C}_6\text{F}_5)]^+$ is an effective CO_2 hydrosilylation catalyst, and was also shown to mediate imine hydrogenation catalysis. Cation $[(\text{ITr})\text{Zn}(\text{C}_6\text{F}_5)]^+$, a well-defined air-, water-tolerant Lewis acid available *via* a couple of synthesis steps from commercial available reagents, could be of potential interest in Lewis acid-type transformations requiring broader substrates/medium tolerance.

Experimental section

Material, reagents, and experimental methods

All experiments were performed under inert atmosphere using standard glove box or Schlenk techniques. Solvents were freshly distilled under N_2 following standard procedures or dispensed from a commercial purification system and then stored over 4 Å molecular sieves. Deuterated solvents were used as received and stored over 4 Å molecular sieves. NMR spectra were recorded on Bruker Avance I-300 MHz, Bruker Avance III-400 MHz, Bruker Avance II-500 MHz, and Bruker Avance III-600 MHz spectrometers. NMR chemical shift values were determined relative to the residual protons in C_6D_6 , $\text{C}_6\text{D}_5\text{Br}$ and CD_2Cl_2 as internal reference for ^1H (δ of the most downfield signal = 7.16, 7.29, 5.32 ppm) and $^{13}\text{C}\{^1\text{H}\}$ (δ of the most downfield signal = 128.06, 130.92, 53.84 ppm). Elemental analysis of all complexes were performed at the elemental analysis service of the University of Strasbourg. ZnMe_2 , ZnEt_2 , and $[\text{CPh}_3][\text{B}(\text{C}_6\text{F}_5)_4]$ were obtained from Strem Chemicals. $\text{B}(\text{C}_6\text{F}_5)_3$ was obtained from TCI Europe and recrystallized from cold pentane prior to use. Carbene [ITr] and salt $[\text{IAd-H}][\text{BF}_4]$ were prepared according to literature procedures.^{21,27}

Carbene [IAd]

In a dry box, the salt $[\text{IAd-H}][\text{BF}_4]$ (1.50 g, 3.54 mmol) was dissolved in THF (70 mL). NaH (128 mg, 5.30 mmol) and a catalytic amount of $t\text{BuOK}$ (39.8 mg, 0.350 mmol) were then added to the mixture, and the reaction flask was vigorously stirred at room temperature overnight. The resulting mixture was then evaporated to dryness under vacuum and the solid residue extracted with toluene (50 mL) and filtered through a Celite pad. Evaporation of the filtrate and subsequent recrystallization of the crude off-white solid (1/1 pentane/toluene mixture,



–30 °C) afforded NMR-pure carbene [IAd] (70% yield), which was used as is.²⁸

[(ITr)Zn(Me)₂] (1)

In a dry box, to a stirring solution of [ITr] free carbene (0.600 g, 1.09 mmol) in toluene (10 mL) was added at once (*via* a syringe) ZnMe₂ (100.0 μL, 1.46 mmol, 1.34 eq.), leading to the massive precipitation of a colorless solid after 30 min. Pentane (50 mL) is then added to the mixture followed a filtration through a glass frit. The collected solid is then washed three times with pentane (3 × 15 mL) and dried under vacuum to yield analytically pure adduct **1** (0.549 g, 85% yield). Anal. Calcd for C₄₃H₃₈N₂Zn: N, 4.32; C, 79.68; H, 5.91. Found: N, 4.51; C, 79.45; H 6.04. ¹H NMR (500 MHz, CD₂Cl₂): δ (ppm) 7.34–7.20 (m, 30H, Ar-H), 6.89 (s, 2H, NCHCHN), –2.13 (s, 6H, ZnMe). ¹³C NMR (125 MHz, CD₂Cl₂): δ (ppm) 142.9 (C_{Ar}), 130.6 (C_{Ar}), 128.5 (C_{Ar}), 128.0 (C_{Ar}), 122.1 (C_{Ar}), 78.3 (NCCN), –6.8 (ZnMe).

[(ITr)Zn(Et)₂] (2)

Adduct **2** was prepared following an identical experimental procedure to that used for the synthesis of **1** but using ZnEt₂ as the Zn precursor. Species **2** was isolated in 91% yield, 615 mg. Anal. Calcd for C₄₅H₄₂N₂Zn: N, 4.14; C, 79.93; H 6.26. Found: N, 4.21; C, 80.11; H 6.33. ¹H NMR (500 MHz, C₆D₆): δ (ppm) 7.35–7.34 (d, *J* = 7 Hz, 12H, Ar-H), 7.19–7.14 (m, 12H, Ar-H), 7.10–7.7 (t, *J* = 7 Hz, 6H, Ar-H), 6.58 (s, 2H, NCHCHN), 1.27 (t, *J* = 8 Hz, 6H, Zn(CH₂CH₃)₂), –0.59 (q, *J* = 8.0 Hz, 4H, Zn(CH₂CH₃)₂). ¹³C NMR (125 MHz, C₆D₆): δ (ppm) 199.0 (C_{carbene}), 142.9 (C_{Ar}), 130.6 (C_{Ar}), 128.4 (C_{Ar}), 128.0 (C_{Ar}), 121.7 (C_{Ar}), 78.4 (NCCN), 15.0 (Zn(CH₂CH₃)₂), 7.00 (Zn(CH₂CH₃)₂).

[(IAd)Zn(R)₂] (3, R = Me; 4, R = Et)⁴³

Species **3** and **4** were prepared following identical procedures to those for **1** and **2** starting from [IAd] (100 mg, 0.297 mmol) and ZnR₂ (1.3 equiv.). Yield in **3**: (120 mg, 94%). Yield in **4** (109 mg, 80%). Data for **3**. Anal. Calcd for C₂₇H₃₈N₂Zn: N, 6.48; C, 69.51; H 8.87. Found: N, 6.62; C, 69.34; H 8.73. ¹H NMR (500 MHz, C₆D₆): δ (ppm) 6.64 (s, 2H, NCHCHN), 2.08 (m, 12H, H-Ad), 1.90 (bs, 6H, H-Ad), 1.48 (d, *J* = 13 Hz, 6H, H-Ad), 1.41 (d, *J* = 13 Hz, 6H, H-Ad), 0.10 (s, 6H, ZnMe₂). ¹³C NMR (125 MHz, C₆D₆): δ (ppm) 186.9 (C_{carbene}), 115.8 (NCCN), 58.2 (C_{Ad}), 43.9 (C_{Ad}), 35.9 (C_{Ad}), 30.0 (C_{Ad}), –7.0 (ZnMe₂). The ¹H and ¹³C NMR data for **4** in C₆D₆ matched those reported in the literature.⁴³

[(ITr)Zn(R)][B(C₆F₅)₄] ([5]⁺, R = Me; [6]⁺, R = Et)

To a solution of neutral [(ITr)Zn(R)₂] (adduct **1** or **2**, 0.065 mmol) in PhF (1 mL) was added dropwise a yellow solution of [CPh₃][B(C₆F₅)₄] (0.060 g, 0.065 mmol, 1 equiv.) in PhF (1 mL). The reaction mixture was stirred for 30 min at room temperature, and the solvent was then evaporated under vacuum. The resulting oily residue was triturated with *n*-pentane (3 × 5 mL) affording a colorless solid, which was then dried under vacuum to yield salt [5][B(C₆F₅)₄] or [6][B(C₆F₅)₄] as an analytically pure powder ([5][B(C₆F₅)₄]: 70.5 mg, 84% yield; [6][B(C₆F₅)₄]: 101.4 mg, 92% yield). Data for [5][B

(C₆F₅)₄]. Anal. Calcd for C₆₆H₃₅BF₂₀N₂Zn: N, 2.13; C, 60.41; H 2.69. Found: N, 2.21; C, 60.34; H 2.76. ¹H NMR (500 MHz, CD₂Cl₂): δ (ppm) 7.51–7.40 (m, 18H, ArH), 7.35 (s, 2H, NCHCHN), 7.20–7.15 (m, 12H, ArH), –1.75 (s, 3H, ZnCH₃). ¹³C NMR (125 MHz, CD₂Cl₂): δ (ppm) 171.6 (C_{carbene}), 148.5 (d, *J*_{CF} = 242 Hz, *o*-C₆F₅), 140.8 (C–Ar), 138.6 (d, *J*_{CF} = 250 Hz, *p*-C₆F₅), 136.6 (d, *J*_{CF} = 244 Hz, *m*-C₆F₅), 130.3 (C_{Ar}), 130.0 (C_{Ar}), 129.6 (C_{Ar}), 123.3 (NCCN), 79.3 (CPh₃), –13.2 (ZnCH₃) ppm. ¹⁹F NMR (282 MHz, CD₂Cl₂): δ (ppm) –133.1 (d, *o*-C₆F₅), –163.7 (t, *J*_{FF} = 20.5 Hz, *p*-C₆F₅), –167.6 (t, *J*_{FF} = 18.8 Hz, *m*-C₆F₅). Data for [6][B(C₆F₅)₄]. Anal. Calcd for C₆₇H₃₇BF₂₀N₂Zn: N, 2.11; C, 60.38; H 2.81. Found: N, 2.15; C, 60.53; H 2.95. ¹H NMR (500 MHz, CD₂Cl₂): δ (ppm) 7.49–7.41 (m, 18H, ArH), 7.32 (s, 2H, NCHCHN), 7.17–7.12 (m, 12H, ArH), 0.23 (t, *J* = 8.1 Hz, 3H, Zn(CH₂CH₃)), –0.86 (q, *J* = 8.1 Hz, 2H, Zn(CH₂CH₃)₂). ¹³C NMR (125 MHz, CD₂Cl₂): δ (ppm) 172.6 (C_{carbene}), 148.5 (d, *J*_{CF} = 241 Hz, *o*-C₆F₅), 141.0 (C–Ar), 138.6 (d, *J*_{CF} = 241 Hz, *p*-C₆F₅), 136.6 (d, *J*_{CF} = 241 Hz, *p*-C₆F₅), 130.2 (C_{Ar}), 130.0 (C_{Ar}), 129.4 (C_{Ar}), 122.7 (NCCN), 79.1 (CPh₃), 10.3 (Zn(CH₂CH₃)₂), 2.6 (Zn(CH₂CH₃)₂). ¹⁹F NMR (282 MHz, CD₂Cl₂): δ (ppm) –133.1 (d, *o*-C₆F₅), –163.8 (t, *J*_{FF} = 20.5 Hz, *p*-C₆F₅), –167.6 (t, *J*_{FF} = 18.8 Hz, *m*-C₆F₅).

[(IAd)Zn(R)][B(C₆F₅)₄] ([7]⁺, R = Me; [8]⁺, R = Et)

To a solution of neutral [(IAd)Zn(R)₂] (adduct **3** or **4**, 0.231 mmol) in PhF (2 mL) was added dropwise a yellow solution of [CPh₃][B(C₆F₅)₄] (213 mg, 0.231 mmol, 1 equiv.) in PhF (1 mL). The reaction mixture was stirred for 1 h at room temperature, and the solvent was then evaporated under vacuum. The resulting oily residue was triturated with *n*-pentane (3 × 5 mL) affording a colorless solid, which was then dried under vacuum to yield salt [7][B(C₆F₅)₄] or [8][B(C₆F₅)₄] as an analytically pure orange powder ([7][B(C₆F₅)₄]: 182 mg, 79% yield; [8][B(C₆F₅)₄]: 198 mg, 84% yield). Data for [7][B(C₆F₅)₄]. Anal. Calcd for C₄₈H₃₅BF₂₀N₂Zn: N, 2.71; C, 55.94; H 3.42. Found: N, 2.62; C, 55.78; H 3.28. ¹H NMR (500 MHz, CD₂Cl₂): δ (ppm) 7.47 (s, 2H, NCHCHN), 2.37 (bs, 6H, HAd), 2.17 (bs, 12H, HAd), 1.88 (bd, *J* = 12.6 Hz, 6H, HAd), 1.76 (bd, *J* = 12.6 Hz, 6H, HAd), 0.01 (s, 3H, ZnMe). ¹³C NMR (125 MHz, CD₂Cl₂): δ (ppm) 155.3 (C_{carbene}), 148.5 (d, *J*_{CF} = 239 Hz), 138.6 (d, *J*_{CF} = 247 Hz), 136.7 (d, *J*_{CF} = 244 Hz), 120.5 (NCCN), 60.1 (CAd), 45.6 (CAd), 35.5 (CAd), 30.1 (CAd), –10.4 (ZnMe). ¹⁹F NMR (282 MHz, CD₂Cl₂): δ (ppm) –133.1 (t, *J*_{FF} = 5 Hz, *o*-C₆F₅), –163.7 (t, *J*_{FF} = 20 Hz, *p*-C₆F₅), –167.5 (t, *J*_{FF} = 13 Hz, *m*-C₆F₅). Data for [8][B(C₆F₅)₄]. Anal. Calcd for C₄₉H₃₇BF₂₀N₂Zn: N, 2.68; C, 56.33; H 3.57. Found: N, 2.75; C, 56.01; H 3.35. ¹H NMR (500 MHz, CD₂Cl₂): δ (ppm) 7.46 (s, 2H, NCHCHN), 2.37 (bs, 6H, HAd), 2.16 (bs, 12H, HAd), 1.88 (bd, *J* = 12.6 Hz, 6H, HAd), 1.76 (bd, *J* = 12.6 Hz, 6H, HAd), 1.29 (t, *J* = 8.1 Hz, 3H, ZnEt), 0.86 (q, *J* = 8.1 Hz, 2 H, ZnEt). ¹³C NMR (125 MHz, CD₂Cl₂): δ (ppm) 155.5 (C_{carbene}), 148.5 (d, *J*_{CF} = 241 Hz), 138.6 (d, *J*_{CF} = 242 Hz), 136.7 (d, *J*_{CF} = 242 Hz), 120.4 (NCCN), 59.9 (CAd), 45.6 (CAd), 35.6 (CAd), 30.2 (CAd), 11.0 (ZnEt), 3.7 (ZnEt) ppm. ¹⁹F NMR (282 MHz, CD₂Cl₂): δ (ppm) –133.1 (t, *J*_{FF} = 5 Hz, *o*-C₆F₅), –163.7 (t, *J*_{FF} = 20.4 Hz, *p*-C₆F₅), –167.6 (t, *J*_{FF} = 18 Hz, *m*-C₆F₅).



$[(\text{ITr})\text{Zn}(\text{C}_6\text{F}_5)][\text{B}(\text{C}_6\text{F}_5)_4] \text{ ([9]B}(\text{C}_6\text{F}_5)_4\text{]}$

A colorless PhF (2 mL) solution of $\text{B}(\text{C}_6\text{F}_5)_3$ (0.300 g, 0.586 mmol, 1.5 equiv.) was added all at once to a solution of $[(\text{ITr})\text{Zn}(\text{Me})][\text{B}(\text{C}_6\text{F}_5)_4]$ (0.250 g, 0.386 mmol, 1 equiv.) in PhF (5 mL). The reaction mixture was stirred for 48 h at room temperature. The volatiles were then evaporated under vacuum and the resulting white solid residue was triturated with *n*-pentane (3 × 5 mL) then dried under vacuum. Recrystallization of the latter from a 1/1 CH_2Cl_2 /pentane mixture stored at -30°C afforded pure $[9]\text{B}(\text{C}_6\text{F}_5)_4$ as a colorless solid (0.501 g, 89% yield). Anal. Calcd for $\text{C}_{71}\text{H}_{32}\text{BF}_{25}\text{N}_2\text{Zn}$: N, 2.00; C, 60.96; H 2.30. Found: N, 2.09; C, 60.71; H 2.43. ^1H NMR (500 MHz, CD_2Cl_2): δ (ppm) 7.50–7.37 (m, 20H, ArH for 18H and NCHCHN for 2H), 7.26–7.18 (m, 12H, ArH). ^{13}C NMR (125 MHz, CD_2Cl_2): δ (ppm) 166.4 ($\text{C}_{\text{carbene}}$), 148.5 (d, $J_{\text{CF}} = 242.0$ Hz, *o*- C_6F_5), 140.3 (C-Ar), 138.6 (d, $J_{\text{CF}} = 243.5$ Hz, *p*- C_6F_5), 136.7 (d, $J_{\text{CF}} = 245$ Hz, *m*- C_6F_5), 130.7 (CAr), 130.5 (CAr), 129.2 (CAr), 125.6 (NCCN), 79.4 (CPh₃). ^{19}F NMR (282 MHz, CD_2Cl_2): δ (ppm) -114.2 to -114.4 (m, Zn-*o*- C_6F_5), -133.1 (d, *o*- $\text{B}(\text{C}_6\text{F}_5)_4$), -152.0 (t, $J_{\text{FF}} = 19.4$ Hz, Zn-*p*- C_6F_5), -160.4 to -160.8 (m, Zn-*m*- C_6F_5), -163.8 (t, $J_{\text{FF}} = 20.4$ Hz, *p*- $\text{B}(\text{C}_6\text{F}_5)_4$), -167.60 (t, *m*- $\text{B}(\text{C}_6\text{F}_5)_4$).

Generation of the water cationic adduct $[(\text{ITr})\text{Zn}(\text{C}_6\text{F}_5)(\text{OH}_2)][\text{B}(\text{C}_6\text{F}_5)_4]$ ($[\mathbf{10}]\text{B}(\text{C}_6\text{F}_5)_4$)

In a dry box, in a vial sample, $[9]\text{B}(\text{C}_6\text{F}_5)_4$ (32.5 mg, 0.022 mmol) was dissolved in $\text{C}_6\text{D}_5\text{Br}$ (0.5 mL) and a stoichiometric amount of H_2O (0.4 μL , 0.022 mmol) was then added. The resulting colorless solution was quickly stirred, transferred to a J-Young-type NMR tube and it was immediately analyzed by ^1H NMR spectroscopy showing the quantitative formation of water cationic adduct $[(\text{ITr})\text{Zn}(\text{C}_6\text{F}_5)(\text{OH}_2)][\text{B}(\text{C}_6\text{F}_5)_4]$ ($[\mathbf{10}]\text{B}(\text{C}_6\text{F}_5)_4$). ^{13}C , ^{19}F , 2D HSQC and 2D HMBC NMR data are all consistent with the proposed formulation (see ESI[†]). ^1H NMR data of $[\mathbf{10}]\text{B}(\text{C}_6\text{F}_5)_4$, as monitored over the course of a month, showed no change indicating the remarkable stability of such Zn(II) organocation at room temperature. ^1H NMR (500 MHz, $\text{C}_6\text{D}_5\text{Br}$): δ (ppm) 7.15–7.10 (t, 12H, ArH), 7.05–6.91 (m, 18H, ArH), 6.83 (s, 2H, NCHCHN), 2.33 (s, 2H, Zn- OH_2). ^{13}C NMR (125 MHz, CD_2Cl_2): δ (ppm) 168.8 ($\text{C}_{\text{carbene}}$), 148.5 (d, $J_{\text{CF}} = 242.0$ Hz, *o*- C_6F_5), 147.8 (d, $J_{\text{CF}} = 242.0$ Hz, Zn- C_6F_5), 140.0 (C-Ar), 138.6 (d, $J_{\text{CF}} = 243.5$ Hz, *p*- C_6F_5), 136.7 (d, $J_{\text{CF}} = 245$ Hz, *m*- C_6F_5), 130.7 (CAr), 130.5 (CAr), 129.2 (CAr), 122.2 (NCCN), 78.8 (CPh₃). ^{19}F NMR (282 MHz, CD_2Cl_2): δ (ppm) -116.1 to -116.25 (m, Zn-*o*- C_6F_5), -131.6 (d, *o*- $\text{B}(\text{C}_6\text{F}_5)_4$), -152.5 (t, $J_{\text{FF}} = 19.4$ Hz, Zn-*p*- C_6F_5), -159.9 (m, Zn-*m*- C_6F_5), -162.0 (t, $J_{\text{FF}} = 20.4$ Hz, *p*- $\text{B}(\text{C}_6\text{F}_5)_4$), -165.8 (t, *m*- $\text{B}(\text{C}_6\text{F}_5)_4$).

Attempted isolation of $[\mathbf{10}]\text{B}(\text{C}_6\text{F}_5)_4$

In a vial sample, $[9]\text{B}(\text{C}_6\text{F}_5)_4$ (65.2 mg, 0.044 mmol) was dissolved in PhBr (2 mL) and a stoichiometric amount of H_2O (0.8 μL , 0.044 mmol) was then added. The resulting colorless solution was stirred for 30 min and evaporated to dryness under vacuum to afford a colorless solid, identified as the starting salt $[9]\text{B}(\text{C}_6\text{F}_5)_4$. Attempted crystallization of the

water adduct $[\mathbf{10}]\text{B}(\text{C}_6\text{F}_5)_4$ through various solvent diffusion approaches (and no evaporation) remained unsuccessful.

 $\{[(\text{ITr})\text{Zn}(\mu\text{-OH})]_2\}[\text{B}(\text{C}_6\text{F}_5)_4]_2$ $[\mathbf{11}]\text{B}(\text{C}_6\text{F}_5)_4]_2$

In a dry box, the water adduct $[(\text{ITr})\text{Zn}(\text{C}_6\text{F}_5)(\text{OH}_2)][\text{B}(\text{C}_6\text{F}_5)_4]$ (0.022 mmol) was *in situ* generated as described above on a NMR scale. The capped NMR tube containing a $\text{C}_6\text{D}_5\text{Br}$ (0.5 mL) of $[\mathbf{10}]\text{B}(\text{C}_6\text{F}_5)_4$ was then heated at 60°C for 24 h. ^1H and ^{19}F NMR analysis agree with the presence of a 1/1 $\text{C}_6\text{F}_5\text{H}/[\mathbf{10}]\text{B}(\text{C}_6\text{F}_5)_4$ mixture, in line with a 50% hydrolysis of the Zn- C_6F_5 bond of the starting $[\mathbf{10}]\text{B}(\text{C}_6\text{F}_5)_4$. Evaporation of the crude mixture and crystallization of the residue from CH_2Cl_2 /pentane solvent layers led the crystallization of $[\mathbf{11}]\text{B}(\text{C}_6\text{F}_5)_4]_2$ (28% yield), whose identity was established by single crystal XRD and elemental analysis data. The obtainment of NMR data for once crystallized $[\mathbf{11}]\text{B}(\text{C}_6\text{F}_5)_4]_2$ was not possible due to its poor solubility. Anal. Calcd for $\text{C}_{130}\text{H}_{66}\text{B}_{24}\text{F}_{40}\text{N}_4\text{O}_2\text{Zn}_2$: N, 2.24; C, 62.41; H 2.66. Found: N, 2.35; C, 62.76; H 2.87.

Author contributions

Xuejuan Xu, Jordan Parmentier: experimental work; Christophe Gourlaouen: DFT calculations and analysis. Béatrice Jacques, Samuel Dagorne: supervision, conceptualization, funding acquisition, data curation; formal analysis, writing – review & editing.

Data availability

The data that support the findings of this study are available in the ESI[†] of this article.

Conflicts of interest

The authors declare no competing financial interests.

Acknowledgements

The University of Strasbourg and the CNRS are gratefully acknowledged for financial support as well as the Agence Nationale de la Recherche (ANR): ANR project Tu-Zin-Cat (ANR-19-CE07-0020-01). X. X. thanks the Chinese Scholarship Council (CSC) and the Fondation Jean-Marie Lehn for PhD and post-doctoral fellowships, respectively. J. P. thanks the ANR for a PhD fellowship.

References

- S. P. Nolan, *N-Heterocyclic Carbenes*, Wiley-VCH Verlag GmbH & Co. KGaA, 2014.
- W. A. Herrmann, *Angew. Chem., Int. Ed.*, 2002, **41**, 1290–1309.



- 3 D. J. Nelson and S. P. Nolan, *Chem. Soc. Rev.*, 2013, **42**, 6723–6753.
- 4 C. A. Smith, M. R. Narouz, P. A. Lummis, I. Singh, A. Nazemi, C.-H. Li and C. M. Crudden, *Chem. Rev.*, 2019, **119**, 4986–5056.
- 5 Q. Zhao, G. Meng, M. Szostak and S. P. Nolan, *Chem. Rev.*, 2020, **120**, 1981–2048.
- 6 M. N. Hopkinson, C. Richter, M. Schedler and F. Glorius, *Nature*, 2014, **510**, 485–496.
- 7 R. H. Crabtree, *Coord. Chem. Rev.*, 2013, **257**, 755–766.
- 8 M. M. D. Roy, A. A. Omaña, A. S. S. Wilson, M. S. Hill, S. Aldridge and E. Rivard, *Chem. Rev.*, 2021, **121**, 12784–12965.
- 9 A. Doddi, M. Peters and M. Tamm, *Chem. Rev.*, 2019, **119**, 6994–7112.
- 10 H. W. Roesky, *J. Organomet. Chem.*, 2013, **730**, 57–62.
- 11 C. Romain, S. Bellemin-Laponnaz and S. Dagorne, *Coord. Chem. Rev.*, 2020, **422**, 213411.
- 12 R. M. Fabicon, A. D. Pajerski and H. G. Richey, *J. Am. Chem. Soc.*, 1991, **113**, 6680–6681.
- 13 P. de Frémont, N. Adet, J. Parmentier, X. Xu, B. Jacques and S. Dagorne, *Coord. Chem. Rev.*, 2022, **469**, 214647.
- 14 D. Specklin, C. Fliedel and S. Dagorne, *Chem. Rec.*, 2021, **21**, 1130–1143.
- 15 S. Dagorne, *Synthesis*, 2018, **50**, 3662–3670.
- 16 M. E. Grundy, K. Yuan, G. S. Nichol and M. J. Ingleson, *Chem. Sci.*, 2021, **12**, 8190–8198.
- 17 A. Rit, A. Zanardi, T. P. Spaniol, L. Maron and J. Okuda, *Angew. Chem., Int. Ed.*, 2014, **53**, 13273–13277.
- 18 R. Guermazi, D. Specklin, C. Gourlaouen, P. de Frémont and S. Dagorne, *Eur. J. Inorg. Chem.*, 2022, **2022**, e202101002.
- 19 D. Specklin, F. Hild, C. Fliedel, C. Gourlaouen, L. F. Veiros and S. Dagorne, *Chem. – Eur. J.*, 2017, **23**, 15908–15912.
- 20 X. Xu, C. Gourlaouen, B. Jacques and S. Dagorne, *Organometallics*, 2023, **42**, 2813–2825.
- 21 M. M. D. Roy, P. A. Lummis, M. J. Ferguson, R. McDonald and E. Rivard, *Chem. – Eur. J.*, 2017, **23**, 11249–11252.
- 22 M. M. D. Roy, M. J. Ferguson, R. McDonald and E. Rivard, *Chem. Commun.*, 2018, **54**, 483–486.
- 23 S. Koop, O. Mrózek, L. Janiak, A. Belyaev, M. Putscher, C. M. Marian and A. Steffen, *Inorg. Chem.*, 2024, **63**, 891–901.
- 24 R. J. Wehmschulte and L. Wojtas, *Inorg. Chem.*, 2011, **50**, 11300–11302.
- 25 T. O. Petersen, D. Simone and I. Crossing, *Chem. – Eur. J.*, 2016, **22**, 15847–15855.
- 26 A. Friedrich, J. Eysel, J. Langer and S. Harder, *Organometallics*, 2021, **40**, 448–457.
- 27 H. Richter, H. Schwertfeger, P. R. Schreiner, R. Fröhlich and F. Glorius, *Synlett*, 2009, 193–197.
- 28 A. J. I. Arduengo, R. L. Harlow and M. Kline, *J. Am. Chem. Soc.*, 1991, **113**, 361–363.
- 29 G. Schnee, C. Fliedel, T. Avilés and S. Dagorne, *Eur. J. Inorg. Chem.*, 2013, **2013**, 3699–3709.
- 30 M. Mantina, A. C. Chamberlin, R. Valero, C. J. Cramer and D. G. Truhlar, *J. Phys. Chem. A*, 2009, **113**, 5806–5812.
- 31 A. D. Horton and J. de With, *Organometallics*, 1997, **16**, 5424–5436.
- 32 D. Tapu, D. A. Dixon and C. Roe, *Chem. Rev.*, 2009, **109**, 3385–3407.
- 33 P. Erdmann, M. Schmitt, L. M. Sigmund, F. Krämer, F. Breher and L. Greb, *Angew. Chem., Int. Ed.*, 2024, **63**, e202403356.
- 34 S. J. Pitman, A. K. Evans, R. T. Ireland, F. Lempriere and L. K. McKemmish, *J. Phys. Chem. A*, 2023, **127**, 10295–10306.
- 35 G. A. N. Felton, A. K. Vannucci, N. Okumura, L. T. Lockett, D. H. Evans, R. S. Glass and D. L. Lichtenberger, *Organometallics*, 2008, **27**, 4671–4679.
- 36 A. Rit, A. Zanardi, T. P. Spaniol, L. Maron and J. Okuda, *Angew. Chem., Int. Ed.*, 2014, **53**, 13273–13277.
- 37 F. J. Fernández-Alvarez and L. A. Oro, *ChemCatChem*, 2018, **10**, 4783–4796.
- 38 P. Jochmann and D. W. Stephan, *Angew. Chem., Int. Ed.*, 2013, **52**, 9831–9835.
- 39 M. Rauch, S. Kar, A. Kumar, L. Avram, L. J. W. Shimon and D. Milstein, *J. Am. Chem. Soc.*, 2020, **142**, 14513–14521.
- 40 S. Paul, P. Morgante, S. N. MacMillan, J. Autschbach and D. C. Lacy, *Chem. – Eur. J.*, 2022, **28**, e202201042.
- 41 P. Mahawar, T. Rajeshkumar, T. P. Spaniol, L. Maron and J. Okuda, *Chem. – Eur. J.*, 2024, **30**, e202401262.
- 42 P. Ji, J. Park, Y. Gu, D. S. Clark and J. F. Hartwig, *Nat. Chem.*, 2021, **13**, 312–318.
- 43 A. J. Arduengo, H. V. R. Dias, F. Davidson and R. L. Harlow, *J. Organomet. Chem.*, 1993, **462**, 13–18.

